

RGBX-R1: Visual Modality Chain-of-Thought Guided Reinforcement Learning for Multimodal Grounding

Jiahe Wu^{1,2,3} Bing Cao¹ Qilong Wang¹ Qinghua Hu¹ Dongdong Li⁴ Pengfei Zhu^{1,2,3}

¹ School of Artificial Intelligence, Tianjin University, Tianjin, China

² Low-Altitude Intelligence Lab, Xiong'an National Innovation Center, Xiong'an, China

³ Xiong'an Guochuang Lantian Technology Co., Ltd., Xiong'an, China

⁴ College of Electronic Science and Technology, National University of Defense Technology, Changsha, China

Abstract

Multimodal Large Language Models (MLLM) are primarily pre-trained on the RGB modality, thereby limiting their performance on other modalities, such as infrared, depth, and event data, which are crucial for complex scenarios. To address this, we propose RGBX-R1, a framework to enhance MLLM's perception and reasoning capacities across various X visual modalities. Specifically, we employ an Understand–Associate–Validate (UAV) prompting strategy to construct the Visual Modality Chain-of-Thought (VM-CoT), which aims to expand the MLLMs' RGB understanding capability into X modalities. To progressively enhance reasoning capabilities, we introduce a two-stage training paradigm: Cold-Start Supervised Fine-Tuning (CS-SFT) and Spatio-Temporal Reinforcement Fine-Tuning (ST-RFT). CS-SFT supervises the reasoning process with the guidance of VM-CoT, equipping the MLLM with fundamental modality cognition. Building upon GRPO, ST-RFT employs a Modality-understanding Spatio-Temporal (MuST) reward to reinforce modality reasoning. Notably, we construct the first RGBX-Grounding benchmark, and extensive experiments verify our superiority in multimodal understanding and spatial perception, outperforming baselines by 22.71% on three RGBX grounding tasks.

1. Introduction

Recently, multimodal large language models (MLLM) [25, 32] demonstrate impressive reasoning capabilities across a wide range of tasks. DeepSeek-R1 [13] proves that reinforcement learning can further enhance the MLLMs' abilities. Subsequent studies [7, 26, 29] validate the applicability of reinforcement learning in multimodal scenarios.

However, the effectiveness of reinforcement learning fundamentally depends on the intrinsic capability of

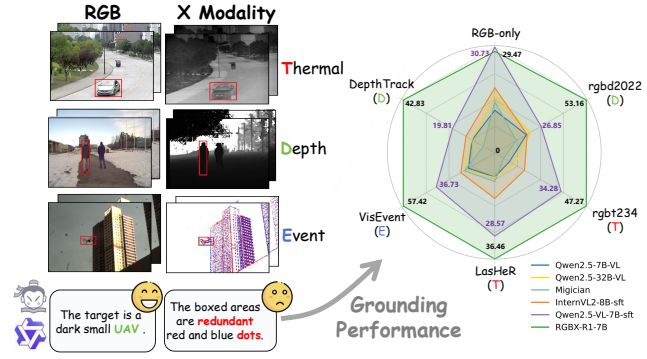


Figure 1. Existing MLLMs exhibit limited capabilities with non-RGB visual modalities and struggle to leverage modality complementarity to enhance multimodal grounding.

MLLMs. Most existing MLLMs are primarily pre-trained on the RGB modality, which limits their ability to generalize beyond RGB-based scenarios. Under degraded conditions—such as nighttime, motion blur, or strong illumination—RGB often becomes unreliable. In contrast, alternative visual modalities, including thermal infrared, depth, and event cameras (collectively referred to as X modalities), exhibit superior robustness under such challenging conditions. Nevertheless, current MLLMs lack the capacity to perceive and reason over these non-RGB modalities, hindering the exploitation of complementary multimodal information for visual understanding in complex environments.

To address these challenges, we propose RGBX-R1, a framework that enhances MLLMs' grounding and reasoning capabilities across diverse visual modalities. RGBX-R1 consists of a cold-start data construction and a two-stage training paradigm. Since MLLMs typically lack prior knowledge of non-RGB modalities, they struggle to explore valid RGBX reasoning paths and cannot directly benefit

from reward-based reinforcement learning. Therefore, it is necessary to first construct cold-start data serving as strong supervision. Specifically, we select RGBX video tracking datasets as the visual source for conducting the cold-start data, as they naturally provide temporally continuous and spatially aligned multimodal data. Following Magician [27], we convert RGBX videos into a multi-image grounding dataset tailored for MLLMs, named *RGBX-Grounding*. Employing RGBX-Grounding as an evaluation benchmark, as shown in Figure 1, it is revealed that even when MLLMs are supervised fine-tuned with bounding boxes, they still struggle to perceive and understand the X modalities effectively. For each RGBX-Grounding sample, we construct a corresponding Visual Modality Chain-of-Thought (VM-CoT) to serve as explicit reasoning annotations within the cold-start data. We design a multi-step prompting strategy—*Understand–Associate–Validate* (UAV)—to transition the MLLM’s RGB cognition to RGBX modality analysis. Employing Qwen2.5-VL-32B [1] as the generator, VM-CoT is produced through the following steps: 1) **Understand** the target based on the RGB modality; 2) **Associate** the X modality with RGB semantics via spatial correspondence; 3) **Validate** the target location by analyzing cross-modal complementarity.

Based on VM-CoT, we perform the two-stage training paradigm. In the first stage, we employ VM-CoT as supervision to guide MLLM’s structured reasoning and establish cognition of the X modality. We incorporate a Modality-specific Token Weighting (MTW) mechanism, enabling the model to prioritize reasoning steps most relevant to the current modality. This stage equips the model with foundational reasoning capabilities and focuses on modeling the intermediate inference process. In the second stage, we extend Group Relative Policy Optimization (GRPO) [28] by introducing a Modality-understanding Spatio-Temporal (MuST) reward mechanism, which comprises three reward components: modality-understanding reward, spatio-temporal reward, and format reward. These rewards jointly encourage the model to comprehend modality-specific cues and accurately ground targets within image sequences. By sampling multiple responses and optimizing the model based on relative advantage, we guide it toward more accurate reasoning behaviors.

We evaluate mainstream MLLMs on the RGBX-Grounding benchmark. Experimental results show that existing MLLMs struggle to understand X modalities and perform poorly on sequential grounding tasks. In contrast, RGBX-R1, empowered by VM-CoT supervision and the two-stage training paradigm, effectively overcomes these limitations. RGBX-R1 outperforms supervised fine-tuned baselines by 22.71% on three RGBX grounding tasks. It is worth noting that RGBX-R1 demonstrates a phenomenon of “*Modal Knowledge Emergent*”, requiring only a small num-

ber of samples to transfer RGB understanding capability to unknown X modalities.

Our contributions can be summarized as follows:

- We propose RGBX-R1, the first multimodal visual reinforcement fine-tuning framework that extends the RGB-based cognition of MLLMs to X modalities, empowering MLLMs with robust multimodal grounding.
- We construct RGBX-Grounding, the first dataset that integrates the generated VM-CoT through the UAV prompting strategy, providing high-quality prior supervision for modality understanding and reasoning.
- We introduce a two-stage training paradigm, CS-SFT and ST-RFT, which employs the MTW mechanism and MuST reward to reinforce reasoning capability. Experiments verify our superiority against the competing MLLMs.

2. Related Work

2.1. Multimodal Grounding

Recent advances in multimodal grounding primarily rely on natural language queries to localize targets in visual scenes [8, 18, 30]. However, language alone provides limited information compared to the rich cues in high-dimensional visual modalities. To address this, the multi-image grounding (MIG) [2, 41] task emerges, using both language instructions and a template image to locate objects across sequences of images. Nevertheless, these methods remain restricted to the RGB modality, making them vulnerable in challenging scenarios where RGB degrades.

In parallel, RGBX tracking [4, 14, 16, 46] shows that integrating complementary visual modalities—irradiance, depth, and event—enhances spatial perception under challenging conditions. Recent efforts [5, 10, 31, 39] further attempt to jointly learn multiple visual modalities through a unified training process. However, these methods remain confined to the visual domain, lacking explicit decision rationales: even when the target is absent or modality signals fail, they still output a location. They overlook the potential of language in bridging visual modalities. In contrast, our work leverages language to explicitly associate RGB and X modalities, enabling interpretable reasoning that captures both modality complementarity and spatial perception.

2.2. Reinforcement Learning in MLLMs

LLMs [6, 11, 12] exhibit strong reasoning capabilities across various tasks. Beyond generating answers, they produce interpretable reasoning steps in natural language through the CoT paradigm [37]. These capabilities allow LLMs to decompose complex problems and explain their decision-making steps. In the multimodal domain, MLLMs extend this reasoning ability by integrating visual inputs, evolving into multimodal CoTs [38, 40, 45].

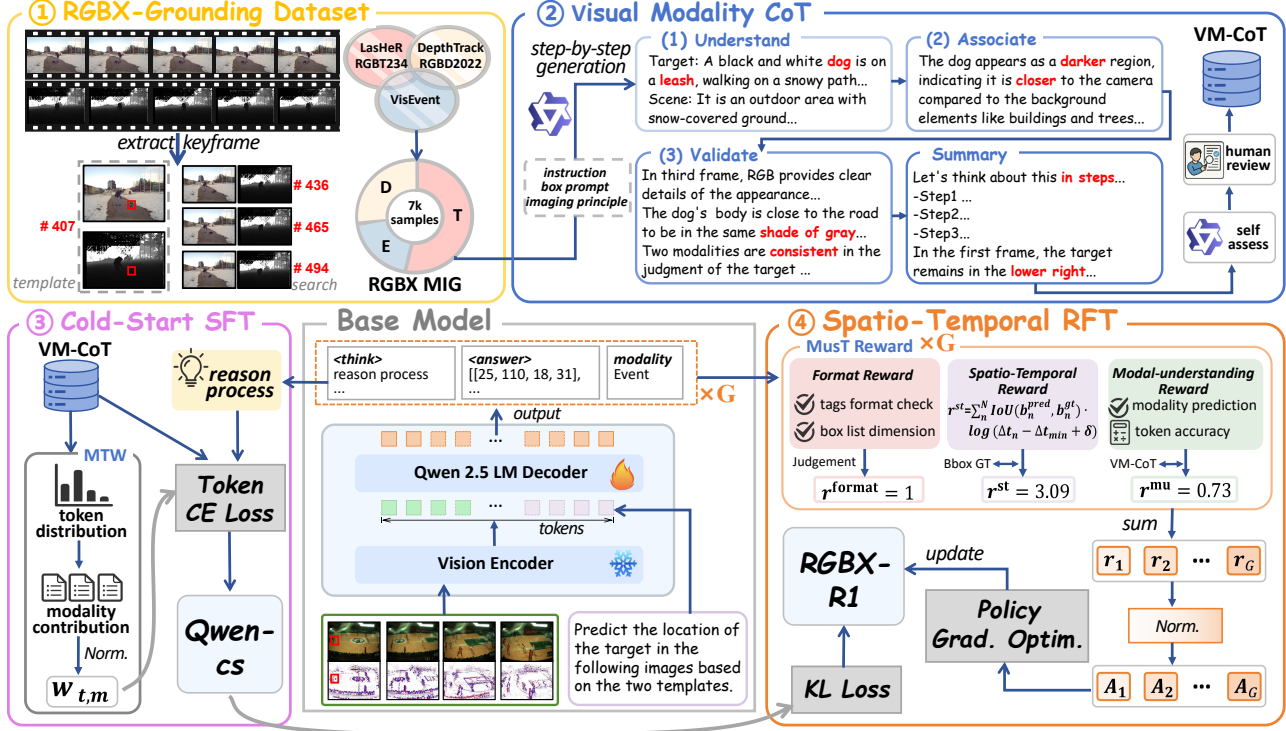


Figure 2. Overall framework of RGBX-R1. (a) RGBX MIG data construction. (b) Constructing VM-CoT with the UAV prompting strategy and two-stage filtering. (c) Cold-start Supervised Fine-Tuning equipped with the MTW mechanism, this stage aims to guide the model in performing structured reasoning. (d) Spatio-Temporal Reinforcement Fine-Tuning. The policy model generates multiple responses and optimizes the model via the MuST group rewards.

Recently, DeepSeek-R1 [13] adopts the GRPO algorithm, which demonstrates that reinforcement learning [21] can significantly enhance the performance of MLLMs. GRPO eliminates the need for trainable reward models by leveraging rule-based numerical rewards. Subsequent studies further validate the effectiveness of reinforcement learning across multimodal reasoning scenarios, including video reasoning [9, 26] and visual grounding [2, 19]. Despite these successes, these methods rely heavily on the MLLMs’ intrinsic reasoning capacity. However, existing MLLMs lack a fundamental understanding of visual modalities beyond RGB, which constrains their reasoning ability in tasks involving more complex modality information. Moreover, current multimodal CoTs [36] are unable to jointly accommodate multiple visual modalities, limiting their ability to provide effective guidance for MLLMs in such tasks.

3. Method

We propose RGBX-R1, a framework designed to enhance the grounding and reasoning capabilities of MLLMs across diverse visual modalities. As shown in Figure 2, RGBX-R1 consists of four main components: RGBX-Grounding dataset construction, VM-CoT generation, Cold-start Su-

pervised Fine-Tuning as the first stage, and Spatio-Temporal Reinforcement Fine-Tuning as the second stage.

3.1. RGBX-Grounding Dataset

Inspired by Magician’s method to process video tracking data, we transform five RGBX tracking datasets [20, 23, 24, 35, 42] into a multi-image grounding (MIG) format. We sample keyframes at intervals of 24 to 29 frames, and every four keyframes produce eight RGBX images, which are grouped into a single MIG sample. In total, we construct 7k sample groups, forming the **RGBX-Grounding** dataset. More details of the dataset are in the Appendix.

Formally, we define the RGBX MIG task as follows: given a language query Q , an RGB target image Z_{RGB} , an X modality target image Z_X , and N search images S as input, the model M output a list of bounding boxes $B \in \mathbb{R}^{N \times 4}$, defined as $B = M(Q, Z_{RGB}, Z_X, S)$. In our dataset, N typically is set to 6.

3.2. Visual Modality CoT

High-quality supervision is critical for guiding model reasoning. Accordingly, we construct VM-CoT annotations for samples in the RGBX-Grounding dataset, serving as structured reasoning supervision during the cold start stage. We

employ Qwen2.5-VL-32B to generate step-by-step reasoning traces under the guidance of predefined prompts and bounding box prompts. The generation follows a three-step pipeline, where the output of each step is incorporated into the prompt for the next step:

- **Understand.** Given an RGB template image, the model understands the target’s semantics and the scene context based on the RGB modality.
- **Associate.** Provided the paired RGB and X modality template images, along with an explanation of the X modality’s imaging principle. Leveraging spatial correspondence derived from the bounding box, the model links the target identified in the RGB modality to its counterpart in the X modality.
- **Validate.** Subsequent search images are analyzed frame by frame to determine whether any modality suffers from information degradation. The model leverages cross-modal complementary information to validate the target’s spatial location.

Finally, the outputs from the three reasoning steps are aggregated and fed back into Qwen2.5-VL-32B to produce a structured summary, producing a unified VM-CoT. To ensure the quality, we adopt a two-stage filtering process. First, the model self-assesses the plausibility of its reasoning based on the ground-truth bounding boxes. Then, we perform a human review to further remove logically flawed cases. While some VM-CoTs may contain errors in details, we believe that they still provide coherent reasoning chains that can guide the model on how to think. In total, we retain more than 5,000 VM-CoTs as high-quality annotations.

3.3. Cold-Start Supervised Fine-Tuning

In the first training stage, we perform Cold-Start Supervised Fine-Tuning (CS-SFT) on Qwen2.5-VL with VM-CoTs, enabling it to conduct structured reasoning following our predefined UAV path. The input prompt explicitly specifies the type of X modality, and the VM-CoT serves as the supervision signal under modality-known conditions.

The reasoning process in RGBX grounding typically involves long-form textual generation, and the VM-CoT often contains many generic words (e.g., “object”, “image”) and structural expressions (e.g., “therefore”, “let me think”), which contribute little to actual modality reasoning. More critically, as different modalities emphasize distinct semantic cues, the contribution of each token to reasoning should vary across modalities. To address this, we introduce a Modality-specific Token Weighting (MTW) mechanism. By measuring the distributional differences of each token across modalities, we estimate its reasoning contribution for the specific modality. For a token t , we calculate its frequency across all VM-CoTs of the current modality m , yielding a normalized distribution $P_m(t)$. We then compute an aggregated mixture distribution $Q_{m'}(t)$ over all other

modalities m' . The modality-specific contribution score of token t , denoted as $\text{Contrib}(t, m)$, is quantified via the KL divergence, as Eq.(10):

$$\text{Contrib}(t, m) = P_m(t) \cdot \log \left(\frac{P_m(t)}{Q_{m'}(t)} \right). \quad (1)$$

A higher divergence indicates that the token carries stronger modality-specific information and is more critical in the reasoning process of modality m . In CS-SFT, we compute the token-level cross-entropy loss between the generated reasoning process and the target VM-CoT. For each token, its contribution score $\text{Contrib}(t, m)$ is normalized within its modality m to obtain the weight $w_{t,m}$, which is used to reweight the loss:

$$\mathcal{L}_{\text{sft}} = - \sum_{t=1}^T w_{t,m} \cdot \log p_\theta(y_t | y_{<t}, x_m), \quad (2)$$

where T denotes the total number of tokens in the VM-CoT, and y_t represents the target token at the t -th position.

3.4. Spatio-Temporal Reinforcement Fine-Tuning

After the first-stage training, the model, referred to as Qwen-*cs*, acquires foundational modality understanding and step-by-step reasoning along the UAV path. In the second stage, we perform Spatio-Temporal Reinforcement Fine-tuning (ST-RFT) on Qwen-*cs*, and adopt the GRPO algorithm to evaluate the quality of responses. Given a query q , the policy π_θ samples a group of G candidate responses $\mathcal{O} = \{o_1, o_2, \dots, o_G\}$, and assigns corresponding rewards $\{r_1, r_2, \dots, r_G\}$ based on predefined rules. To encourage accurate modality understanding and precise grounding, we propose the MuST reward mechanism, which decomposes the overall reward r into three components: Spatio-Temporal reward r^{st} , Modality-understanding reward r^{mu} and Format reward r^{format} .

Spatio-Temporal Reward. We observe that MLLMs often exhibit a phenomenon we refer to as “*Inertial Numeric Guessing*” when predicting sequences of bounding boxes. Specifically, the MLLM tends to generate coordinate sequences that deviate from actual visual content, often showing numeric progressions or oscillation patterns around the initial coordinates. To mitigate this, we design the Spatio-Temporal Reward r^{st} by incorporating frame-aware weighting to the IoU-based reward, which emphasizes accurate grounding in later frames while reducing the impact of coincidental correctness in earlier ones:

$$r^{\text{st}} = \sum_{n=1}^N \log_{10} (\Delta t_n - \Delta t_{\min} + \delta) \cdot \text{IoU}(b_n^{\text{pred}}, b_n^{\text{gt}}), \quad (3)$$

where Δt_n is the frame interval between the n -th image and the template, and Δt_{\min} is the minimum frame interval in the sequence. IoU denotes Intersection over Union metric.

Modality-understanding Reward. We incorporate a proportion of modality-unknown samples during training. For these samples, the model is required to additionally perform modality classification. If the predicted modality is correct, we compute the reward r^{mu} based on the mean token accuracy of the reasoning process enclosed in `<think></think>`, compared against the VM-CoT. For correctly classified cases, r^{mu} typically ranges between 0.6 and 0.9. If classification is wrong, $r^{\text{mu}} = 0$.

Format Reward. This reward ensures that the response of the model strictly follows the required format, producing the corresponding content within the delimiters and matching the list dimensions: `<think>thinking process</think> <answer> B ∈ ℝN × 4</answer>`. If the format is correct, $r^{\text{format}} = 1$. Otherwise, $r^{\text{format}} = 0$.

The final reward for the response o_i is computed as $r_i = r^{\text{mu}} + r^{\text{st}} + r^{\text{format}}$. Then we compute the group-normalized advantage \hat{A}_i with reward standardization:

$$\hat{A}_i = \frac{r_i - \text{mean}(\{r_i\}_{i=1}^G)}{\text{std}(\{r_i\}_{i=1}^G)}. \quad (4)$$

The objective of GRPO updates the policy π_θ by maximizing the expected \hat{A}_i , encouraging the generation of responses with higher quality. The objective also considers preventing the optimized policy π_θ from deviating far from the Qwen-CoT π_{ref} by a KL-divergence term $\mathbb{D}_{\text{KL}}(\cdot \parallel \cdot)$:

$$\max_{\theta} \mathbb{E}_{q, \{o_i\} \sim \pi_\theta^{\text{old}}} \left[\frac{1}{G} \sum_{i=1}^G \frac{1}{|o_i|} \sum_{t=1}^{|o_i|} \text{clip}(r_{i,t}(\theta), 1 \pm \epsilon) \hat{A}_{i,t} \right] - \beta \cdot \mathbb{D}_{\text{KL}}(\pi_\theta \parallel \pi_{\text{ref}}), \quad (5)$$

$$r_{i,t}(\theta) = \frac{\pi_\theta(o_{i,t} \mid q, o_{i,<t})}{\pi_\theta^{\text{old}}(o_{i,t} \mid q, o_{i,<t})}, \quad (6)$$

where β is a hyperparameter of KL regularization towards the reference model. By leveraging these advantages, the model is optimized toward more accurate reasoning.

4. Experiments

4.1. Experimental Setup

Dataset. The dataset RGBX-Grounding is constructed from five RGBX tracking datasets as the image sources: Vi-sEvent [35] for the event modality, DepthTrack [42] and RGBD2022 [20] for the depth modality, RGBT234 [23] and LasHer [24] for the thermal infrared modality. RGBX-Grounding contains a total of 7,432 samples and 59k images. Detailed statistics are provided in the Appendix.

Evaluation Metrics. The evaluation on RGBX-Grounding adopts the traditional metric Acc@0.5, which measures grounding accuracy. A prediction is considered correct if its IoU with the ground truth is greater than 0.5. The final score is computed by equally averaging correctness across all frames in a sequence. Evaluation adopts two settings: modality-known and modality-unknown, based on whether the type of modality is specified in input prompts.

Implementation Details. RGBX-R1 is developed based on Qwen2.5-VL-Instruct as the base model, and we conduct experiments with both the 3B and 7B versions. In the first stage, we train for 3 epochs on the full RGBX-Grounding dataset, resulting in Qwen-*cs*. In the second stage, we sample from the dataset and designate 20% of the samples as modality-unknown (with prompts referring to X modality). We then perform 1,500 steps of reinforcement learning, obtaining the final RGBX-R1 model. For the final version, the hyperparameters are set as $G = 8$, $\beta = 0.05$, and $\delta = 5$. The maximum generation length is set to 2,048. All experiments are performed on NVIDIA RTX A6000 GPUs.

Baselines. Our baseline models can be categorized into the following groups: (1) Basic MLLMs, including LLaVA-OV-7B [22], InternVL2-8B [3], and Qwen2.5-VL [1] ranging from 3B to 32B, where the 32B model serves as the generator for VM-CoT. We also incorporated the closed-source model Qwen3-Plus [43]. (2) Models fine-tuned for multi-image grounding tasks, including Magician [27] and UniVG-R1 [2]. (3) Supervised fine-tuned baselines: we fine-tune Qwen2.5-VL-7B and InternVL2-8B on RGBX-Grounding for supervised fine-tuning, denoted as Qwen2.5-VL-7B-*sft* and InternVL2-8B-*sft*. We also perform a second-stage training on Qwen2.5-VL-7B-*sft* employing the same ST-RFT as applied to RGBX-R1, denoted as Qwen2.5-VL-7B-*sft+st*.

4.2. Overall Performance

RGBX Grounding. Table 9 presents the RGBX grounding performance comparison between our method and the baselines. Our method includes the first-stage-only model (-*cs*), second-stage-only model (-*sft*) and the two stage model (RGBX-R1). To ensure that the baselines can understand the task and input information, we design task-specific prompts for each MLLM and perform evaluation under modality-known conditions. As shown in Table 9, the grounding performance of several 7B-scale MLLMs remains below 20%. Even the Qwen-2.5-VL-32B model, which serves as the VM-CoT generator, performs poorly without an explicit reasoning prompt. UniVG-R1 [2] fails to comprehend the task and cannot generate answers in sequence format. In contrast, RGBX-R1 achieves substantial improvements across all evaluation subsets. After two-stage training, RGBX-R1 outperforms the supervised fine-tuning baselines, with improvements of 15.45%,

Table 1. Performance comparison on the RGBX-Grounding, including models ranging from 3B to 32B in scale, and the closed-source model. Two models (-*sft*) serve as the primary baselines, along with Qwen at different training stages as the ablation study.

Method	Thermal		Depth		Avg.	X-total
	LasHeR	RGBT.	DepthT.	RGBD.		
Qwen2.5-VL-32B [1]	8.33	10.34	10.76	20.70	19.13	13.24
Qwen3-Plus [43]	15.73	13.62	13.49	21.88	20.96	16.59
Qwen2.5-VL-3B [1]	5.87	3.59	5.05	8.59	11.22	7.70
Qwen2.5-VL-3B- <i>cs</i>	9.07	11.35	11.29	12.89	22.38	14.67
RGBX-R1-3B	26.71	32.76	25.32	34.38	38.36	31.70
LLaVA-OV-7B [22]	1.78	1.47	1.58	0.78	8.44	4.22
InternVL2-8B [3]	8.67	6.47	7.38	10.16	18.85	12.24
Qwen2.5-VL-7B [1]	8.25	7.61	10.65	18.36	16.51	11.90
Migician- [27]	9.84	4.60	5.38	12.50	19.07	12.47
InternVL2-8B- <i>sft</i>	15.61	15.37	17.83	18.75	22.36	17.60
Qwen2.5-VL-7B- <i>sft</i>	28.57	34.28	19.81	26.56	36.73	31.04
Qwen2.5-VL-7B- <i>cs</i>	14.66	17.67	19.30	23.04	25.08	19.64
Qwen2.5-VL-7B- <i>st</i>	25.14	30.15	14.55	16.87	22.74	23.19
Qwen2.5-VL-7B- <i>sft+st</i>	29.75	39.86	22.24	24.05	38.98	32.74
RGBX-R1-7B	36.46	47.27	42.83	53.16	57.42	46.53

25.43%, and 23.69% on the three modality tasks compared to Qwen2.5-VL-*sft*, and 26.37%, 31.87%, and 36.11% compared to InternVL2-*sft*. Even with the 3B model, RGBX-R1 surpasses the 7B-*sft* baselines.

Single Modality Grounding. To assess the discrimination capability of different MLLMs for the RGB and X modalities, we further evaluate the 7B-scale models using a single modality. We adopt modality-unknown prompts and provide either RGB or X images as input. As shown in Table 2, “RGB” denotes using only RGB inputs across all subsets, while “X-total” denotes using only the corresponding X modality. When relying solely on RGB, RGBX-R1 outperforms Qwen2.5-VL-7B by 17.74%, attributed to the Spatio-Temporal reward improving sequential coordinate prediction. RGBX-R1 lags behind the baseline Qwen2.5-VL-7B-*sft* by 1.96%. When relying solely on the X modality, RGBX-R1 surpasses Qwen2.5-VL-7B-*sft* by 15.83%, 11.63%, and 8.58% across the three modalities, and exceeds the pretrained model by 17.01% in total. In contrast, Qwen2.5-VL-7B-*sft* improves over the pretrained model by 16.91% when using only RGB, but by merely 4.54% when using only X. These results indicate that training solely with coordinate supervision provides limited capability for effective perception of the unknown X modality.

4.3. Discussion

Training Stage. Table 9 presents the impact of different training stages on the grounding performance. RGBX-R1 achieves an average improvement of 26.89% compared to the first-stage-only Qwen2.5-VL-7B-*cs*, demonstrating the complementary benefits of the two-stage training pipeline. When using only the second stage, the per-

Table 2. Performance comparison of 7B-scale models under unimodal inputs with unknown types.

Method	RGB	Thermal	Depth	Event	X-total
Qwen2.5-VL	12.82	5.67	6.13	10.44	7.54
Migician	14.90	6.23	4.89	11.86	8.19
InternVL2- <i>sft</i>	18.93	9.64	7.17	11.86	10.12
Qwen2.5-VL- <i>sft</i>	32.48	12.30	7.44	13.57	12.08
RGBX-R1	30.56	28.13	16.08	22.15	24.55

Table 3. Ablation study of the MTW mechanism on RGBX-R1-7B across the two training stages.

Version	MTW	Grounding			Rensoning	
		Th.	De.	Ev.	TA.	Mu.
Qwen2.5-VL- <i>cs</i>		13.64	17.08	22.74	64.15	-
Qwen2.5-VL- <i>cs</i>	✓	13.82	18.07	23.08	62.39	-
RGBX-R1		36.95	36.73	55.65	-	75.51
RGBX-R1	✓	39.31	42.05	57.06	-	79.62

mance of Qwen2.5-VL-7B-*st* is even lower than Qwen2.5-VL-7B-*sft* on the Depth and Event modalities and exhibits a 23.40% overall performance drop compared to the two-stage RGBX-R1. This gap underscores the necessity of the cold start with the VM-CoT. Compared to the baseline Qwen2.5-VL-7B-*sft+st* that combines conventional SFT and ST-RFT, RGBX-R1 has achieved comprehensive improvements, with an average increase of 13.79%. This improvement is attributed to the supervision of the reasoning process by VM-CoT.

MTW Mechanism. We conduct an ablation study on the MTW mechanism to evaluate its impact on both grounding and reasoning performance across four model variants, as shown in Table 3. To measure reasoning performance, we adopt the mean token accuracy (TA.) as the metric for the first-stage model (-*cs*), and adopt the mean Modality-understanding reward (Mu.) over the last 50 steps for two-stage models. As shown in Table 3, the MTW mechanism consistently improves grounding performance in both stages, with a more pronounced gain in the complete two-stage model. Moreover, incorporating MTW in the first stage does not affect the training stability. Even when evaluated by mean token accuracy, the model with MTW shows only a drop of 1.76%. In practice, its reasoning ability becomes more modality-specialized, which translates into stronger grounding capability.

MuST Reward. The ablation studies on the reward mechanism under modality-unknown evaluation are presented in Table 7. **Case 4** represents the complete MuST reward mechanism. **Case 1** demonstrates that the Format reward, serving as the fundamental reward, largely determines the overall effectiveness of training. The performance on the event modalities in Case 1 is even inferior to

Table 4. Ablation study of reward mechanisms on the grounding performance of RGBX-R1-7B.

	r_{format}	r_{mu}	r_{st}	r_{mi}	Thermal	Depth	Event	Total
Case 1		✓	✓		26.81	25.24	23.70	25.41
Case 2	✓		✓		37.89	34.63	52.18	42.83
Case 3	✓	✓		✓	35.43	41.68	54.67	43.62
Case 4	✓	✓	✓		39.31	42.05	57.06	46.43

Table 5. Ablation study of the training data scale.

Sample	Modality-known			Modality-unknown			
	Size	Thermal	Depth	Event	Thermal	Depth	Event
base		8.13	12.28	16.51	8.11	10.76	15.60
1%		24.87	30.37	28.59	24.43	28.58	27.18
10%		33.67	43.21	44.12	33.57	37.09	42.36
Full		38.17	45.90	57.42	39.31	42.05	57.06

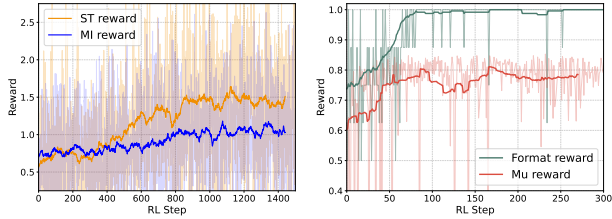


Figure 3. The curves of rewards during ST-RFT.

Qwen2.5-VL-7B-*cs*. In **Case 2**, the depth modality is most affected without r_{mu} , showing a 7.42% drop compared to Case 4. In **Case 3**, we replaced our Spatio-Temporal (ST) reward r_{st} with the Mean IoU (MI) reward r_{mi} , which computes the mean IoU value of all predicted bounding boxes as the reward. ST reward leads to an average 2.81% improvement in grounding accuracy. Furthermore, we visualize the evolution of the MuST reward throughout reinforcement steps, applying smoothing to the curves in Figure 3. The results confirm that the ST reward facilitates more precise grounding than the MI reward. The Modality-understanding (Mu) reward and Format reward converge within around 200 steps, and the overall training stabilizes around 1,500 steps.

Modality Contribution. In Figure 4, we illustrate the impact of the RGB and X modalities on grounding performance. The dashed lines represent evaluations under modality-unknown conditions. Across all five subsets, using solely RGB consistently outperforms using only the X modality, with this advantage highlighted in deep purple. The light purple segments highlight the superiority of joint RGB and X modality, where the model leverages complementary information from both modalities to achieve more robust grounding than using either modality alone. Interestingly, in both thermal infrared datasets, modality-unknown inference slightly exceeds modality-known inference. We

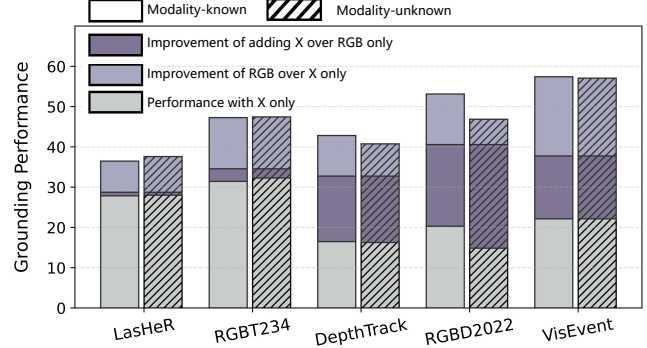


Figure 4. Grounding performance of RGBX-R1-7B under different modality inputs to illustrate modality contributions.

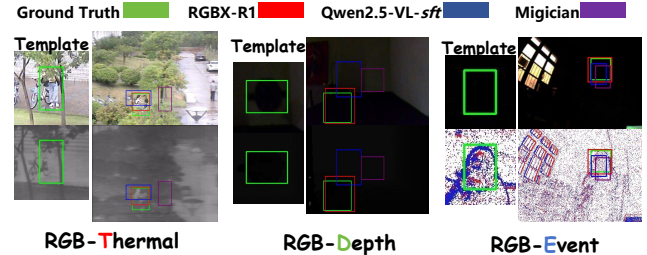


Figure 5. Visualization of RGBX grounding results. The green rectangles indicate targets in the template images.

attribute this to richer cross-modal reasoning triggered by the absence of explicit types of X modalities.

Sample Scale. We present the effect of training data scale on RGBX-R1’s grounding performance in Table 8. We adopt uniform sampling when utilizing only 1% and 10% of the total samples. At the 1% level, each modality includes an average of merely 20 multi-image combinations. Remarkably, even with such a small fraction of data, RGBX-R1 achieves a significant enhancement over the baseline Qwen2.5-VL-7B. With 10% of the data, the performance on the depth modality already approximates that obtained with the full dataset. These results underscore that our method, even with a minimal number of RGBX samples, can effectively elicit the model’s understanding of previously unknown X modalities and conduct modal complementary analysis. Such performance exhibits a strong property of “*Modal Knowledge Emergent*”.

4.4. Qualitative Evaluation

Grounding Result. We visualize the qualitative results of our method and other approaches, as shown in Figure 5. All methods are evaluated using 7B scale models. While competing methods struggle under degraded conditions, RGBX-R1 consistently maintains robust grounding performance, benefiting from its enhanced understanding of the X modality and cross-modal complementary reasoning. In

Question:

A sequence of images consisting of alternating modalities. Your task is to predict the coordinates of the target object in the subsequent images after the first two template images, based on the green bounding boxes `<box>` `</box>` in templates.

RGB-THERMAL

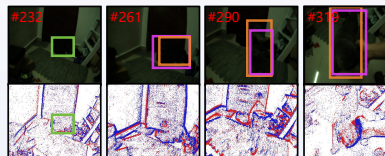


RGBX-R1:

<think>
Step 1: ...one potted **cactus**... man in a hooded jacket crouches nearby...
Dracaena... center; **fern**... right...
Step 2: ...pot exhibits elevated temperature...cactus itself shows significantly **higher temperature** than the other two plants...
Step 3: RGB modality... Clearly distinguishes all three plants... **Infrared**... cactus displays notably **high grayscale**... Both modalities reflect the **same** target area, confirming... the cactus is **moved** to the center position, **swapping** places with the Dracaena...
</think>

<answer>
shown as **orange** boxes above.
</answer>

RGB-EVENT



RGBX-R1:

<think>
Step 1: The target is a **dark cat**...
Step 2: ...identify modality...event uses **red and blue dots** to indicate changes in **pixel brightness**...
Second Group: ...cat's body **blends** into the dark wooden door in RGB... In event, concentrated **red dots** form a **circular** pattern, suggesting **head movement** adjustments...
Third Group...**validating** target presence...
Step 3: ...Both modalities indicate **consistent localization** of the cat...
Summarizing the position... In the last pair, the cat is **picked up** by a person...
</think>

<answer>
shown as **orange** boxes above.
</answer>

RGB-DEPTH



RGBX-R1:

<think>
Step 1: The target is the **duck** closest to the shore...several ducks are farther...
Step 2: ...It should be the **depth**...the sky background shows higher grayscale values...the target has **lower grayscale**...
...second image set... the depth modality suffers from severe **noise**, and the corresponding region does not reveal a clear duck **contour**...
Step 3: ...The duck consistently **remains** at the position closest to the shore... In the depth image, the corresponding region exhibits a **noticeable contrast** change in grayscale values, **validating**...
</think>

<answer>
shown as **orange** boxes above.
</answer>

Figure 6. An example of RGBX-R1-7B’s reasoning outputs, with reasoning keywords highlighted in bold and specific color. In the images, green, purple and orange boxes denote the input information, the ground truth and the prediction, respectively.

the RGB-Event case, where the RGB modality completely fails, other methods can only estimate the target’s location based on its initial position in the template images. Magician exhibits the “*Inertial Numeric Guessing*” phenomenon in all three cases, deviating from the actual visual content and solely relying on the initial coordinates for prediction. In the RGB-Depth case, even when both modalities suffer from degradation, our method still successfully grounds the target. Furthermore, our RGBX-R1 also has a more precise grounding capability, framing the entire object rather than partial regions.

Reasoning Process. In Figure 6, we present three representative reasoning examples of RGBX-R1-7B across diverse modalities, showcasing its structured multi-step reasoning process. The model consistently follows the intended reasoning path, beginning with comprehensive target understanding, proceeding through fine-grained frame-by-frame modality analysis, and culminating in a synthesized estimation of the target’s spatial location. Throughout this process, RGBX-R1 actively leverages modality-

specific characteristics for both supplementation and cross-checking—illustrated by reasoning segments such as “*validating target presence*” and “*indicating consistent localization*.” This explicit integration of cross-modal cues enables the model to refine its spatial perception and significantly bolster grounding robustness. Additional visualization results and reasoning examples are provided in the Appendix.

5. Conclusion

In this paper, we present RGBX-R1, a framework that empowers MLLMs with enhanced grounding and reasoning capabilities across diverse visual modalities. RGBX-R1 first leverages the VM-CoT to provide structured reasoning supervision for Cold-Start Supervised Fine-Tuning, equipping the model with fundamental modality understanding with the aid of the MTW mechanism. Building upon GRPO, Spatio-Temporal Reinforcement Fine-Tuning employs the MuST reward to reinforce spatio-temporal perception and modality reasoning. Extensive experiments on our

proposed RGBX-Grounding benchmark demonstrate substantial improvements over strong baselines, confirming the effectiveness of our approach in complex and degraded multimodal grounding scenarios. To the best of our knowledge, RGBX-R1 is the first multimodal visual reinforcement fine-tuning framework to explore MLLMs' reasoning capabilities for RGBX grounding tasks, establishing a new task paradigm and benchmark for future work.

References

- [1] Shuai Bai, Keqin Chen, Xuejing Liu, Jialin Wang, Wenbin Ge, Sibo Song, Kai Dang, Peng Wang, Shijie Wang, Jun Tang, et al. Qwen2.5-vl technical report. *arXiv preprint arXiv:2502.13923*, 2025. [2](#), [5](#), [6](#)
- [2] Sule Bai, Mingxing Li, Yong Liu, Jing Tang, Haoji Zhang, Lei Sun, Xiangxiang Chu, and Yansong Tang. Univg-r1: Reasoning guided universal visual grounding with reinforcement learning. *arXiv preprint arXiv:2505.14231*, 2025. [2](#), [3](#), [5](#)
- [3] Zheng Cai, Maosong Cao, Haojong Chen, Kai Chen, Keyu Chen, Xin Chen, Xun Chen, Zehui Chen, Zhi Chen, Pei Chu, et al. Internlm2 technical report. *arXiv preprint arXiv:2403.17297*, 2024. [5](#), [6](#)
- [4] Bing Cao, Junliang Guo, Pengfei Zhu, and Qinghua Hu. Bi-directional adapter for multimodal tracking. In *Proceedings of the AAAI Conference on Artificial Intelligence*, pages 927–935, 2024. [2](#)
- [5] Xin Chen, Ben Kang, Wanting Geng, Jiawen Zhu, Yi Liu, Dong Wang, and Huchuan Lu. Sutrack: Towards simple and unified single object tracking. In *Proceedings of the AAAI Conference on Artificial Intelligence*, pages 2239–2247, 2025. [2](#), [1](#)
- [6] Hyung Won Chung, Le Hou, Shayne Longpre, Barret Zoph, Yi Tay, William Fedus, Yunxuan Li, Xuezhi Wang, Mostafa Dehghani, Siddhartha Brahma, et al. Scaling instruction-finetuned language models. *Journal of Machine Learning Research*, 25(70):1–53, 2024. [2](#)
- [7] Jisheng Dang, Jingze Wu, Teng Wang, Xuanhui Lin, Nannan Zhu, Hongbo Chen, Wei-Shi Zheng, Meng Wang, and Tat-Seng Chua. Reinforcing video reasoning with focused thinking. *arXiv preprint arXiv:2505.24718*, 2025. [1](#)
- [8] Jiajun Deng, Zhengyuan Yang, Daqing Liu, Tianlang Chen, Wengang Zhou, Yanyong Zhang, Houqiang Li, and Wanli Ouyang. Transvg++: End-to-end visual grounding with language conditioned vision transformer. *IEEE Transactions on Pattern Analysis and Machine Intelligence*, 45(11):13636–13652, 2023. [2](#)
- [9] Kaituo Feng, Kaixiong Gong, Bohao Li, Zonghao Guo, Yibing Wang, Tianshuo Peng, Junfei Wu, Xiaoying Zhang, Benyou Wang, and Xiangyu Yue. Video-r1: Reinforcing video reasoning in mllms. *arXiv preprint arXiv:2503.21776*, 2025. [3](#)
- [10] Xiaokun Feng, Dailing Zhang, Shiyu Hu, Xuchen Li, Meiqi Wu, Jing Zhang, Xiaotang Chen, and Kaiqi Huang. Cstrack: Enhancing rgb-x tracking via compact spatiotemporal features. *arXiv preprint arXiv:2505.19434*, 2025. [2](#)
- [11] Luciano Floridi and Massimo Chiriatti. Gpt-3: Its nature, scope, limits, and consequences. *Minds and machines*, 30(4):681–694, 2020. [2](#)
- [12] Aaron Grattafiori, Abhimanyu Dubey, Abhinav Jauhri, Abhinav Pandey, Abhishek Kadian, Ahmad Al-Dahle, Aiesha Letman, Akhil Mathur, Alan Schelten, Alex Vaughan, et al. The llama 3 herd of models. *arXiv preprint arXiv:2407.21783*, 2024. [2](#)
- [13] Daya Guo, Dejian Yang, Haowei Zhang, Junxiao Song, Ruoyu Zhang, Runxin Xu, Qihao Zhu, Shirong Ma, Peiyi Wang, Xiao Bi, et al. Deepseek-r1: Incentivizing reasoning capability in llms via reinforcement learning. *arXiv preprint arXiv:2501.12948*, 2025. [1](#), [3](#)
- [14] Lingyi Hong, Shilin Yan, Renrui Zhang, Wanyun Li, Xinyu Zhou, Pinxue Guo, Kaixun Jiang, Yiting Chen, Jinglun Li, Zhaoyu Chen, et al. Onetracker: Unifying visual object tracking with foundation models and efficient tuning. In *Proceedings of the IEEE/CVF Conference on Computer Vision and Pattern Recognition*, pages 19079–19091, 2024. [2](#)
- [15] Xiaojun Hou, Jiazheng Xing, Yijie Qian, Yaowei Guo, Shuo Xin, Junhao Chen, Kai Tang, Mengmeng Wang, Zhengkai Jiang, Liang Liu, et al. Sdstrack: Self-distillation symmetric adapter learning for multi-modal visual object tracking. In *Proceedings of the IEEE/CVF Conference on Computer Vision and Pattern Recognition*, pages 26551–26561, 2024. [1](#)
- [16] Xiantao Hu, Ying Tai, Xu Zhao, Chen Zhao, Zhenyu Zhang, Jun Li, Bineng Zhong, and Jian Yang. Exploiting multimodal spatial-temporal patterns for video object tracking. In *Proceedings of the AAAI Conference on Artificial Intelligence*, pages 3581–3589, 2025. [2](#)
- [17] Xiantao Hu, Ying Tai, Xu Zhao, Chen Zhao, Zhenyu Zhang, Jun Li, Bineng Zhong, and Jian Yang. Exploiting multimodal spatial-temporal patterns for video object tracking. In *Proceedings of the AAAI Conference on Artificial Intelligence*, pages 3581–3589, 2025. [1](#), [2](#)
- [18] Zhong Ji, Jiahe Wu, Yaodong Wang, Aiping Yang, and Jun-gong Han. Progressive semantic reconstruction network for weakly supervised referring expression grounding. *IEEE Transactions on Circuits and Systems for Video Technology*, 34(12):13058–13070, 2024. [2](#)
- [19] Qing Jiang, Xingyu Chen, Zhaoyang Zeng, Junzhi Yu, and Lei Zhang. Rex-thinker: Grounded object referring via chain-of-thought reasoning. *arXiv preprint arXiv:2506.04034*, 2025. [3](#)
- [20] Matej Kristan, Aleš Leonardis, Jiří Matas, Michael Felsberg, Roman Pflugfelder, Jóni-Kristian Kämäräinen, Hyung Jin Chang, Martin Danelljan, Luka Čehovin Zajc, Alan Lukežić, et al. The tenth visual object tracking vot2022 challenge results. In *European Conference on Computer Vision*, pages 431–460. Springer, 2022. [3](#), [5](#)
- [21] Aviral Kumar, Vincent Zhuang, Rishabh Agarwal, Yi Su, John D Co-Reyes, Avi Singh, Kate Baumli, Shariq Iqbal, Colton Bishop, Rebecca Roelofs, et al. Training language models to self-correct via reinforcement learning. *arXiv preprint arXiv:2409.12917*, 2024. [3](#)
- [22] Bo Li, Yuanhan Zhang, Dong Guo, Renrui Zhang, Feng Li, Hao Zhang, Kaichen Zhang, Peiyuan Zhang, Yanwei Li, Zi-

wei Liu, et al. Llava-onevision: Easy visual task transfer. *arXiv preprint arXiv:2408.03326*, 2024. 5, 6

[23] Chenglong Li, Xinyan Liang, Yijuan Lu, Nan Zhao, and Jin Tang. Rgb-t object tracking: Benchmark and baseline. *Pattern Recognition*, 96:106977, 2019. 3, 5

[24] Chenglong Li, Wanlin Xue, Yaqing Jia, Zhichen Qu, Bin Luo, Jin Tang, and Dengdi Sun. Lasher: A large-scale high-diversity benchmark for rgbt tracking. *IEEE Transactions on Image Processing*, 31:392–404, 2021. 3, 5

[25] Feng Li, Renrui Zhang, Hao Zhang, Yuanhan Zhang, Bo Li, Wei Li, Zejun Ma, and Chunyuan Li. Llava-next-interleave: Tackling multi-image, video, and 3d in large multimodal models. *arXiv preprint arXiv:2407.07895*, 2024. 1

[26] Xinhao Li, Ziang Yan, Desen Meng, Lu Dong, Xiangyu Zeng, Yinan He, Yali Wang, Yu Qiao, Yi Wang, and Limin Wang. Videochat-r1: Enhancing spatio-temporal perception via reinforcement fine-tuning. *arXiv preprint arXiv:2504.06958*, 2025. 1, 3

[27] You Li, Heyu Huang, Chi Chen, Kaiyu Huang, Chao Huang, Zonghao Guo, Zhiyuan Liu, Jinan Xu, Yuhua Li, Ruixuan Li, et al. Magician: Revealing the magic of free-form multi-image grounding in multimodal large language models. *arXiv preprint arXiv:2501.05767*, 2025. 2, 5, 6

[28] Zhihong Shao, Peiyi Wang, Qihao Zhu, Runxin Xu, Junxiao Song, Xiao Bi, Haowei Zhang, Mingchuan Zhang, YK Li, Yang Wu, et al. Deepseekmath: Pushing the limits of mathematical reasoning in open language models. *arXiv preprint arXiv:2402.03300*, 2024. 2

[29] Haozhan Shen, Peng Liu, Jingcheng Li, Chunxin Fang, Yibo Ma, Jiajia Liao, Qiaoli Shen, Zilun Zhang, Kangjia Zhao, Qianqian Zhang, et al. Vlm-r1: A stable and generalizable r1-style large vision-language model. *arXiv preprint arXiv:2504.07615*, 2025. 1

[30] Wei Su, Peihai Miao, Huanzhang Dou, Gaoang Wang, Liang Qiao, Zheyang Li, and Xi Li. Language adaptive weight generation for multi-task visual grounding. In *Proceedings of the IEEE/CVF Conference on Computer Vision and Pattern Recognition*, pages 10857–10866, 2023. 2

[31] Yuedong Tan, Zongwei Wu, Yuqian Fu, Zhuyun Zhou, Guolei Sun, Eduard Zamfi, Chao Ma, Danda Pani Paudel, Luc Van Gool, and Radu Timofte. Xtrack: Multimodal training boosts rgbd video object trackers. *arXiv preprint arXiv:2405.17773*, 2024. 2

[32] Gemini Team, Petko Georgiev, Ving Ian Lei, Ryan Burnell, Libin Bai, Anmol Gulati, Garrett Tanzer, Damien Vincent, Zhufeng Pan, Shibo Wang, et al. Gemini 1.5: Unlocking multimodal understanding across millions of tokens of context. *arXiv preprint arXiv:2403.05530*, 2024. 1

[33] Yunjie Tian, Lingxi Xie, Jihao Qiu, Jianbin Jiao, Yaowei Wang, Qi Tian, and Qixiang Ye. Fast-itpn: Integrally pre-trained transformer pyramid network with token migration. *IEEE Transactions on Pattern Analysis and Machine Intelligence*, 2024. 1

[34] Ramakrishna Vedantam, C Lawrence Zitnick, and Devi Parikh. Cider: Consensus-based image description evaluation. In *Proceedings of the IEEE conference on computer vision and pattern recognition*, pages 4566–4575, 2015. 3

[35] Xiao Wang, Jianing Li, Lin Zhu, Zhipeng Zhang, Zhe Chen, Xin Li, Yaowei Wang, Yonghong Tian, and Feng Wu. Visevent: Reliable object tracking via collaboration of frame and event flows. *IEEE Transactions on Cybernetics*, 54(3):1997–2010, 2023. 3, 5

[36] Yaoting Wang, Shengqiong Wu, Yuecheng Zhang, Shuicheng Yan, Ziwei Liu, Jiebo Luo, and Hao Fei. Multimodal chain-of-thought reasoning: A comprehensive survey. *arXiv preprint arXiv:2503.12605*, 2025. 3

[37] Jason Wei, Xuezhi Wang, Dale Schuurmans, Maarten Bosma, Fei Xia, Ed Chi, Quoc V Le, Denny Zhou, et al. Chain-of-thought prompting elicits reasoning in large language models. *Advances in Neural Information Processing Systems*, 35:24824–24837, 2022. 2

[38] Lai Wei, Wenkai Wang, Xiaoyu Shen, Yu Xie, Zhihao Fan, Xiaojin Zhang, Zhongyu Wei, and Wei Chen. Mc-cot: A modular collaborative cot framework for zero-shot medical-vqa with llm and mllm integration. *arXiv preprint arXiv:2410.04521*, 2024. 2

[39] Zongwei Wu, Jilai Zheng, Xiangxuan Ren, Florin-Alexandru Vasluiianu, Chao Ma, Danda Pani Paudel, Luc Van Gool, and Radu Timofte. Single-model and any-modality for video object tracking. In *Proceedings of the IEEE/CVF Conference on Computer Vision and Pattern Recognition*, pages 19156–19166, 2024. 2, 1

[40] Guowei Xu, Peng Jin, Ziang Wu, Hao Li, Yibing Song, Lichao Sun, and Li Yuan. Llava-cot: Let vision language models reason step-by-step. In *Proceedings of the IEEE/CVF International Conference on Computer Vision*, pages 2087–2098, 2025. 2

[41] Yunqiu Xu, Linchao Zhu, and Yi Yang. Mc-bench: A benchmark for multi-context visual grounding in the era of mllms. *arXiv preprint arXiv:2410.12332*, 2024. 2

[42] Song Yan, Jinyu Yang, Jani Käpylä, Feng Zheng, Aleš Leonardis, and Joni-Kristian Kämäräinen. Depthtrack: Unveiling the power of rgbd tracking. In *Proceedings of the IEEE/CVF International Conference on Computer Vision*, pages 10725–10733, 2021. 3, 5

[43] An Yang, Anfeng Li, Baosong Yang, Beichen Zhang, Binyuan Hui, Bo Zheng, Bowen Yu, Chang Gao, Chengen Huang, Chenxu Lv, et al. Qwen3 technical report. *arXiv preprint arXiv:2505.09388*, 2025. 5, 6

[44] Botao Ye, Hong Chang, Bingpeng Ma, Shiguang Shan, and Xilin Chen. Joint feature learning and relation modeling for tracking: A one-stream framework. In *European conference on computer vision*, pages 341–357. Springer, 2022. 1

[45] Zhuosheng Zhang, Aston Zhang, Mu Li, Hai Zhao, George Karypis, and Alex Smola. Multimodal chain-of-thought reasoning in language models. *arXiv preprint arXiv:2302.00923*, 2023. 2

[46] Jiawen Zhu, Simiao Lai, Xin Chen, Dong Wang, and Huchuan Lu. Visual prompt multi-modal tracking. In *Proceedings of the IEEE/CVF Conference on Computer Vision and Pattern Recognition*, pages 9516–9526, 2023. 2, 1

RGBX-R1: Visual Modality Chain-of-Thought Guided Reinforcement Learning for Multimodal Grounding

Supplementary Material

1. RGBX-Grounding Dataset

RGBX-Grounding covers three modality-specific tasks, sampling image data from five RGBX datasets: VisEvent for the event modality, DepthTrack and RGBD2022 for the depth modality, and RGBT234 and LasHeR for the thermal infrared modality. To extract keyframes, we select specific frames at an interval of 24 to 29 frames in most cases, depending on the total frame count of each original video. However, a small portion of videos in VisEvent, LasHeR, and RGBT234 contain fewer than 80 frames. For these short videos, we adopt a unified minimum interval corresponding to 13 frames. Such short videos account for less than 1% of the dataset. In RGBX-Grounding, 97.24% of the samples consist of two template images followed by six search images for grounding. Additionally, 2.28% and 0.48% of the samples solely contain six and four images, respectively. To maintain a balanced distribution of data samples, we extract at most 8 sample groups of multi-image grounding from each video, avoiding excessive samples from videos exceeding 2,000 frames. For training and testing splits, we follow the original splits of VisEvent, DepthTrack, and LasHeR to partition our multi-image samples. Since RGBD2022 and RGBT234 do not provide predefined splits, we perform our own partitioning. In total, RGBX-Grounding comprises 7,432 multi-image grounding samples, with more than 58k images. Detailed statistics are provided in Table 6.

Table 6. Statistics of the RGBX-Grounding dataset.

Image Numbers	Thermal		Depth		Event
	33,082		11,216		
Subset	LasHeR	RGBT234	DepthTrack	RGBD2022	VisEvent
Train Samples	2,615	522	732	366	1,096
Test Samples	826	175	240	65	795

2. Performance of RGBX Tracking Methods

We evaluate RGBX video object tracking methods [5, 15, 17, 39, 46] on our proposed RGBX-Grounding benchmark. SUTrack and Un-Track are selected as representative methods. We use their official checkpoints, models trained on the original RGBX video datasets, to perform our multi-image grounding task. Their grounding performance results are presented in Table 7, marked with *. It should be noted that the training samples from only three original RGBX video datasets—LasHeR, DepthTrack, and VisEvent—amount to 1,894k, which is 32 times larger than the

Table 7. Grounding performance of RGBX video tracking methods on RGBX-Grounding.

	RGBT234	RGBD2022	VisEvent	AVG.
Trained on original video data				
Un-Track* [39]	60.58	61.18	51.65	53.76
SUTrack_b224* [5]	64.16	62.70	53.87	56.16
Trained on RGBX-Grounding				
ViPT [46]	46.34	39.36	46.11	45.72
Un-Track [39]	47.28	38.49	46.59	46.19
SDSTrack [15]	48.05	39.78	46.61	46.42
STTrack [17]	49.96	42.73	46.75	47.04
SUTrack_t224 [5]	49.16	40.09	46.78	46.74
SUTrack_b224 [5]	50.44	40.47	46.92	47.11
RGBX-R1	47.27	53.16	57.42	55.43

Table 8. Grounding performance of RGBX video tracking methods on RGBX-Grounding with 1% data scale.

	RGBT234	RGBD2022	VisEvent	AVG.
ViPT	19.62	17.62	12.61	14.11
Un-Track	19.47	17.90	12.84	14.27
STTrack	20.37	19.26	16.97	17.69
SUTrack_t224	22.13	17.89	13.99	15.61
SUTrack_b224	22.46	18.37	15.28	16.69
RGBX-R1	24.43	28.58	27.18	26.80

RGBX-Grounding dataset. Moreover, their training samples are temporally continuous. The results indicate that the frame-sampled data from RGBX-Grounding presents a more challenging grounding task compared to the original continuous data, exhibiting a performance degradation of 20%-30% compared to the evaluations [5, 39] conducted on the original video dataset. This is primarily because, in the multi-image grounding paradigm, targets may undergo substantial displacement between frames, which poses a greater challenge to a model’s capabilities in target identification and relational reasoning.

For a fair comparison, we retrained these RGBX trackers on the RGBX-Grounding training data using the pre-trained weights of the backbone networks [33, 44]. The results are summarized in Table 7. Among these, only SUTrack [5] and our RGBX-R1 utilize modality-mixed samples for a single training session, whereas other approaches are trained and evaluated under modality-specific conditions. The results show that our RGBX-R1 achieves the best average performance across the three X-modal grounding tasks, outperforming the second-best SUTrack_b224 by an average

of 8.32%. However, these RGBX trackers generally exhibit better grounding performance in the thermal infrared modality, with SUTrack_b224 surpassing our RGBX-R1 by 3.17%. The performance advantage of RGBX-R1 is most pronounced in the depth modality, where it exceeds the sub-optimal SUTrack_b224 by 12.69%.

Additionally, to evaluate the cross-modal transfer capability of these RGBX trackers under extreme few-shot settings, we retrained them using only 1% of modality-balanced samples. As shown in Table 8, we trained with only 1% of the training samples and evaluated on the full test set. On the three RGBX grounding tasks, our method demonstrates a more significant performance advantage, surpassing the best RGBX tracker, STTrack [17], by 4.06%, 9.32%, and 10.21%, respectively.

3. Prompts in UAV Prompting Strategy

We annotate reasoning processes for all training samples in RGBX-Grounding. Using Qwen2.5-VL-Instruct-32B as the generator, we employ the UAV prompting strategy to produce the Visual Modality Chain-of-Thought (VM-CoT) by 4 steps in total. The first three steps correspond to the three stages of the UAV strategy, while the final step reformats and summarizes the outputs from these steps to produce the final VM-CoT. In the UAV strategy, each step’s prompt consists of multiple sub-prompts, including {task prompt}, {modality prompt}, {previous-step answer prompt}, and {current-step prompt}. The {previous-step answer prompt} incorporates the generator’s output from the preceding step. The prompts for the first three steps follow the sub-prompt structure described below:

- **Step-1.** {task prompt} + {current-step prompt}.
- **Step-2.** {task prompt} + {modality prompt} + {previous-step answer prompt} + {current-step prompt}.
- **Step-3.** {task prompt} + {modality prompt} + {previous-step answer prompt} + {current-step prompt}.

The specific sub-prompt content is presented below. The {task prompt}, which aims to guide the model to understand the input format and the final task objective. The {} denotes the specific parameters to be passed. The {task prompt} is as follows:

A total of {num} images are provided, consisting of alternating RGB and {modality} images. Each RGB image is paired with the subsequent {modality} image, which is spatially and temporally aligned. The final task is to predict the target’s location in each of the subsequent images, based on the target marked by the green bounding box. Green box coordinates: {box}.

The {modality prompt} provides the imaging principle of the X modality as prior knowledge:

- **Thermal:** *The thermal infrared modality is based on temperature sensing. Regions with higher temperatures have higher grayscale values, appearing white or light*

gray; conversely, lower temperatures appear as dark gray or black. For example, a pedestrian target in the RGB modality exhibits a higher temperature and appears as a gray-white human-shaped region in the infrared modality, while cooler backgrounds such as roads appear black.

- **Depth:** *The depth modality is based on the distance of objects from the camera. The closer an object is to the viewpoint, the lower its grayscale value, appearing dark gray or black; the farther it is, the whiter it appears. For instance, if the target is a ball positioned near the camera, it appears as a dark circular region in the depth modality.*
- **Event:** *The event modality is based on changes in pixel intensity. A response is triggered only when brightness increases or decreases beyond a threshold, with red indicating increased intensity and blue indicating decreased intensity. For example, the headlights of a car in the RGB modality appear as small circular clusters of red pixels in the event modality, indicating the emergence of a brighter object in that region.*

Below are the {current-step prompt} used in each step of the UAV strategy, where {example} denotes a carefully designed fixed example provided as guidance for each step:

- **Understand:** *Using only the RGB modality, describe the target inside the green box, along with any other objects or scene context related to the target (if applicable). For example, {example}.*
- **Associate:** *Establish spatial correspondence between the two modalities. Based on the RGB modality and the description of the last step, interpret the target information at the corresponding positions in each modality image. Here is the principle of {modality}: {modality prompt}. For example, {example}. The reasoning process for this step should not exceed 200 words.*
- **Validate:** *First, analyze the complementary relationship between the two modalities in target grounding. Specifically, for each image, determine whether one modality experiences information degradation and whether the other modality provides complementary cues. Avoid general statements about modality contribution—perform image-specific analysis. Finally, verify the target location based on the cross-modal complementarity and describe the target position. For example, {example}. The reasoning process for this step should not exceed 400 words.*

Finally, we merge the outputs from the above three steps and feed them back into the generator for structured summarization. During this process, redundant content across the three outputs is filtered out, and a unified format for VM-CoT is produced. After a two-stage filtering process, we retain 5,000 VM-CoTs for the samples in RGBX-Grounding.

4. Modality-specific Token Weighting

In the Modality-specific Token Weighting (MTW) mechanism, we measure the distributional differences of each to-

ken across modalities. Inspired by the CIDEr metric [34], we quantify the importance of tokens for modal reasoning through frequency statistics. Similar to the concept of Term Frequency and Inverse Document Frequency in CIDEr, if a word appears more frequently within the current modality, it is considered more discriminative for that specific modality. Conversely, if a token is common across the VM-CoTs of all modalities, its value is deemed lower. For a token t , we statistics its frequency in all VM-CoTs of the specific modality m , denoted as $f(t, m)$. We then compute its normalized distribution $P_m(t)$ for the current modality m , and the aggregated mixture distribution $Q_m(t)$ over all other modalities m' :

$$P_m(t) = \frac{f(t, m)}{N_m}, \quad (7)$$

$$Q_m(t) = \frac{\sum_{m' \neq m} f(t, m')}{\sum_{m' \neq m} N_{m'}}, \quad (8)$$

where N_m is the total number of tokens of all VM-CoTs in modality m . We then quantify the modality-specific contribution score of token t :

$$\text{Contrib}(t, m) = P_m(t) \cdot \log \left(\frac{P_m(t)}{Q_{m'}(t)} \right). \quad (9)$$

The contribution scores $\text{Contrib}(t, m)$ are normalized separately for each modality. Specifically, we first apply a logarithmic transformation to obtain $L_m(t)$, followed by min–max normalization. Finally, the normalized values are linearly mapped to the range $[0.05, 1]$, denoted as $\alpha_{t,m}$:

$$\alpha_{t,m} = \mu + (1 - \mu) \cdot \frac{\log(\max(\text{Contrib}(t, m), \delta)) - L_{\min}}{L_{\max} - L_{\min} + \varepsilon}, \quad (10)$$

where μ is set to 0.05, and δ and ε are very small positive numbers. $\alpha_{t,m}$ is used as the training loss weights during Cold-Start Supervised Fine-Tuning. The modality-specific weights obtained from MTW are presented in Table 9.

5. Grounding Visualization

In Fig.7, we present the grounding results of RGBX-R1, where two complete multi-image grounding examples are shown for each RGBX modality. Among cases b,d,c,e, various scene degradation phenomena are observed to validate the robustness of our model’s grounding capability.

In case b, the third search image exhibits RGB overexposure, yet the model accurately localizes the target by relying on infrared information. In case c, the search images display sparse depth information because the target and background are at nearly the same distance, causing partial information

Table 9. Modality-specific token weights for each modality. We present a part of tokens with the highest and lowest weights.

Thermal		Event		Depth	
token	weight	token	weight	token	weight
thermal	1.00	event	1.00	depth	1.00
heat	0.97	dots	0.95	camera	0.92
infrared	0.94	blue	0.93	proximity	0.90
signature	0.89	points	0.93	distance	0.87
temperature	0.88	motion	0.92	darker	0.86
cooler	0.87	red	0.91	farther	0.86
bright	0.85	drone	0.90	lighter	0.85
umbrella	0.85	rapid	0.88	background	0.84
warmer	0.83	movement	0.86	closer	0.83
⋮	⋮	⋮	⋮	⋮	⋮
the	0.05	a	0.05	of	0.05

loss. The model combines the blurred RGB view and partial depth contours to estimate the target’s position. In case d, the target has completely moved out of the frame in the second search image. The model infers its approximate disappearance position based on its relative relation to other objects. In case e, motion blur occurs in the second and third search images of the RGB modality. The model relies on the event modality to determine the approximate target position; however, relying solely on the event modality still results in minor grounding bias. In addition, in cases a and f, the model localizes the target with high precision.

6. Reasoning Examples

We present the complete reasoning processes for several representative case studies included in the paper. Fig.8, Fig.9 and Fig.10 correspond to event, thermal infrared, and depth modalities, respectively. From these reasoning processes, RGBX-R1 strictly follows the predefined reasoning path. Building upon a solid understanding of each modality’s characteristics, it leverages cross-modal complementarity to achieve collaborative grounding.

In addition to the correct grounding cases with positive reasoning outcomes, we also examine failure cases to analyze their reasoning processes. As shown in Fig.11, Fig.12 and Fig.13, each presents a negative case from different modalities. According to the IoU@0.5 metric, correct boxes and incorrect ones are marked with green check marks and red crosses, respectively. In Fig.11, due to noise present in both the RGB and event modalities, the model fails to accurately interpret the target semantics. In Fig.12, the target overlaps or swaps positions with visually similar objects, leading to incorrect identification. In Fig.13, in the final search image, both the color contrast in RGB and grayscale contrast in the depth modality are low, causing the model to mistakenly infer that the target has exited the frame.

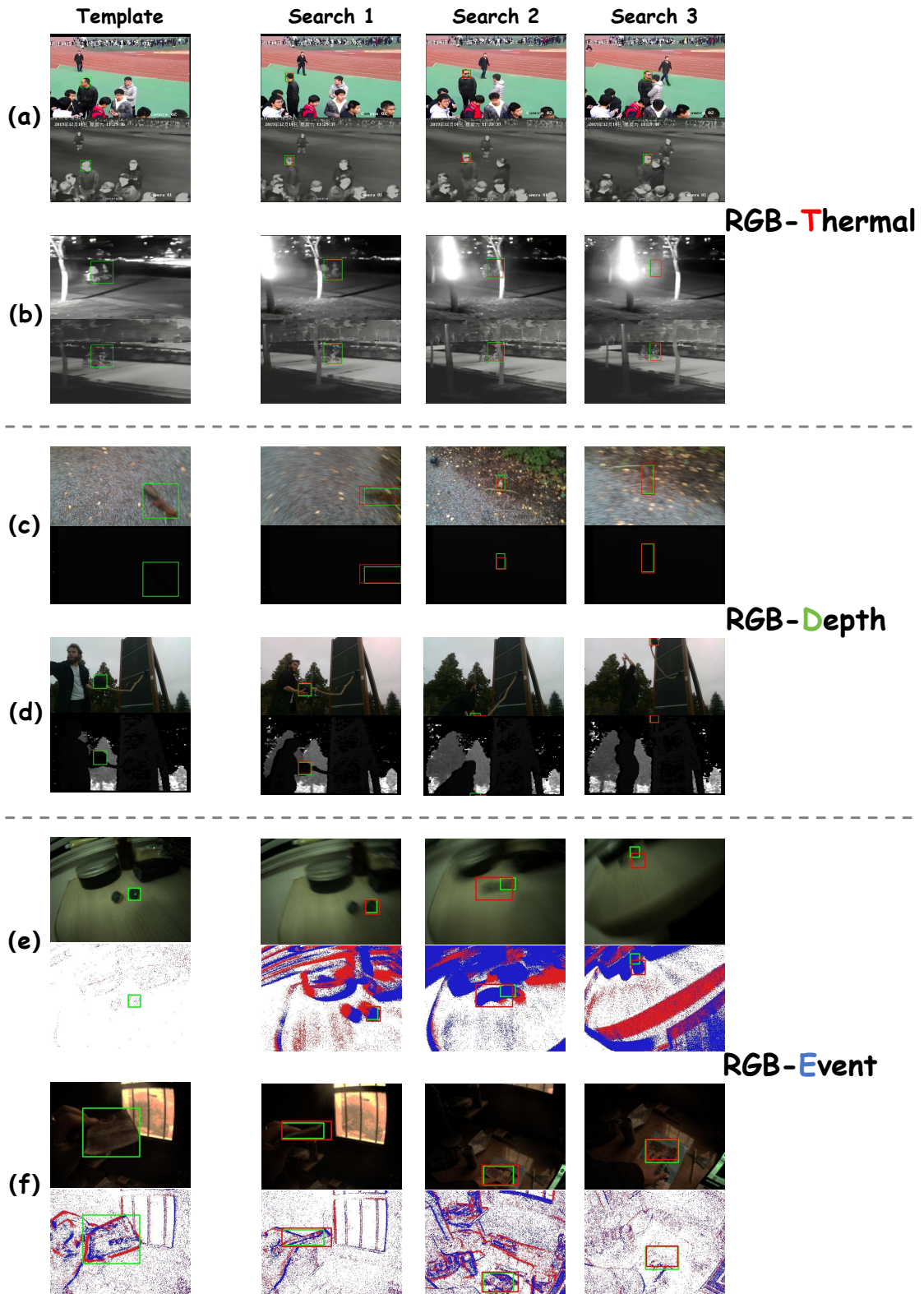
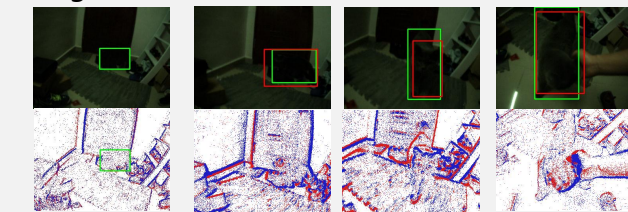


Figure 7. Visualization of RGBX-R1’s grounding results. Green boxes denote ground-truth bounding boxes, while red boxes indicate RGBX-R1’s predictions.

Images:



Question:

A sequence of images has been input, consisting of alternating modalities images. Your task is to predict the coordinates of the target object in the subsequent images after the first two template images, based on the green bounding boxes [168.05,105.59,76.86,53.44] in these two templates.

RGBX-R1-7B:

<think> Step 1: The target in the first two images is a **dark-colored cat** lying on a patterned rug near a door. The scene includes: A dark-colored rug with a striped pattern. A wooden door in the background. Some objects scattered around, such as a blue item (possibly a bag or toy) to the right of the cat. A shelf or cabinet structure on the right side of the image.

Step 2: I need to identify the modality type beyond RGB. The image shows dense **red and blue dots** corresponding to the object's contour. This is consistent with the characteristics of event modality, which uses red and blue dots to indicate rapid changes in **pixel brightness**. Therefore, this should be **[Event Modality]**. **First Group:** RGB: The cat lies on a patterned rug near a door. Its body blends into the dark wooden door above due to **low color contrast**. Event Modality: Dense dots cluster around the cat's body, reflecting subtle movements. **Second Group:** RGB: The cat shifts slightly while maintaining a crouched posture. Event Modality: Concentrated **red dots** form a circular pattern at the original position, suggesting **head movement** adjustments. **Third Group:** RGB: The cat moves across the rug with visible positional offset. Event Modality: The cat's full contour is delineated by sustained event activity, **validating** target presence. **Fourth Group:** RGB: A person lifts the cat, causing posture disruption. Event Modality: High-intensity bursts of event dots occur due to rapid brightness changes from human-cat interaction.

Step 3: RGB: Clearly presents the cat's appearance and visual information of the surrounding environment. However, in low-light conditions or when the cat **blends into the background**, details may become less distinct. Event Modality: Effectively captures brightness changes, highlighting the cat's movements even in low-light scenarios. Positional Consistency: Both modalities indicate **consistent localization** of the cat.

Summarizing the target position. In the next pairs, the cat remains on the rug but its position has slightly moved. In the last pair, the cat is being picked up by a person, as indicated by the close proximity to a human hand and the change in the cat's posture. </think>

<answer>[[177,109,134,93], [177,109,134,93], [175,86,74,142], [175,86,74,142], [102,24,128,197], [102,24,128,197]]</answer>

Answer: [[197.081,110.8671,111.4984,83.4589], [162.4439,56.7673,83.4589,179.4531], [98.7777,0.0,112.1582,234.9009]]

Figure 8. An example reasoning process of correct RGB–Event grounding. The target to be grounded is a cat.

Images:



Question:

A sequence of images has been input, consisting of alternating modalities images. Your task is to predict the coordinates of the target object in the subsequent images after the first two template images, based on the green bounding boxes [282.0,173.0,33.0,48.0] in these two templates.

RGBX-R1-7B:

<think> Step 1: The target is a **potted cactus**. A man in a hooded jacket crouches nearby the roadside is crouching it. In front of him are three potted plants: the cactus on the left, a Dracaena in the center, and a fern on the right. The scene takes place at night on a street, with utility poles along the sidewalk.

Step 2: I need to identify the modality beyond RGB. The modality following RGB appears as a grayscale image, where the person's head and limbs show high grayscale values in sharp contrast to the black road background, indicating the **infrared** modality. In the **first** set of images, the person's body shows high temperature. In addition, the pots exhibit **elevated temperatures**. The cactus has a noticeably **higher temperature** than the other two plants, comparable to its pot. In the **second** set of images, the person is holding the cactus. In the **third** set, the cactus has been **moved** to the middle position, retaining a clear appearance in the infrared view. The fourth set shows the same configuration.

Step 3: In the **RGB** modality, the distinction among all three plants is clear. The cactus has a **spherical** shape that is visually distinct from the leafy forms of the other two. In the **infrared** modality, the cactus shows a distinct high **grayscale value**, second only to the human body. Across the image sets, the cactus is visibly relocated. Both modalities reflect the **same** target area, confirming that the cactus is moved to the center position, **swapping** places with the Dracaena originally on the left. RGB and infrared **jointly verify** this spatial relocation.

In summary, in the second image, the cactus remains in its **initial** position. In the third and fourth images, it has been moved to the middle position, slightly shifted to the **left**. </think>

<answer>[[306,155,34,54], [306,155,34,54], [324,144,36,53], [324,144,36,53], [325,146,34,51], [325,146,34,51]]</answer>

Answer: [[308.0,157.0,35.0,48.0], [325.0,149.0,35.0,46.0], [325.0,149.0,35.0,50.0]]

Figure 9. An example reasoning process of correct RGB–Thermal grounding. The target to be grounded is a pot of cactus.

Images:**Question:**

A sequence of images has been input, consisting of alternating modalities images. Your task is to predict the coordinates of the target object in the subsequent images after the first two template images, based on the green bounding boxes [378,0,158,0,50,0,43,0] in these two templates.

RGBX-R1-7B:

<think> Step 1: The target is the **duck closest** to the shore. At the bottom of the frame is the shoreline, where a pigeon is standing. In the lake, aside from the target duck, there are **three other ducks** positioned slightly farther from the shore, and several more ducks farther away near the top of the frame.

Step 2: I need to identify the modality. The modality is likely **depth**, as the riverside bank in the lower part of the image is **closer** to the camera and appears **black**, while the sky background shows **higher grayscale** values, consistent with the imaging principle of the depth modality. In the **first set** of images, the target duck appears as an **oval light-gray** region in the depth modality at the corresponding location, showing a **lower grayscale value** than the lake surface. However, the depth modality contains some **noise**, resulting in an **unclear target contour**. In the **second set**, the four ducks near the shore maintain their relative positions without significant displacement. The depth modality suffers from severe **noise**, and the corresponding region does not reveal a clear duck contour, roughly appearing as a **parallelogram**. In the **third set**, the target duck turns its head toward the shore. The depth modality shows a **light-gray contour** in the corresponding region, revealing the duck's **pointed tail**. In the **fourth set**, as the duck turns its head, the target in the depth modality also changes shape.

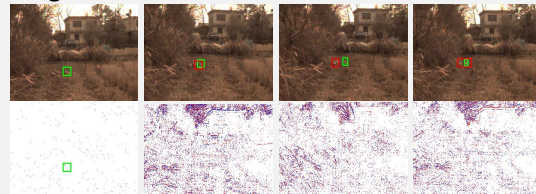
Step 3: Throughout the sequence, the target duck **remains closest** to the shore. In the grayscale depth images, the corresponding RGB positions show distinct grayscale contrast, **confirming** the target's location. The distant ducks also maintain their relative positions without significant displacement, **avoiding confusion** with the target.

In summary, the duck remains in its original position without noticeable displacement, with only changes in **body orientation**. </think>

<answer>[[425,154,55,40], [425,154,55,40], [448,139,34,48], [448,139,34,48], [456,144,64,66], [456,144,64,66]]</answer>

Answer: [[424.0,152.0,58.0,45.0], [443.0,138.0,45.0,48.0], [453.0,151.0,71.0,52.0]]

Figure 10. An example reasoning process of correct RGB–Depth grounding. The target to be grounded is a duck.

Images:**Question:**

A sequence of images has been input, consisting of alternating modalities images. Your task is to predict the coordinates of the target object in the subsequent images after the first two template images, based on the green bounding boxes [143.9827,169.7167,21.2731,22.7507] in these two templates.

RGBX-R1-7B:

<think> Step 1: The target within the green bounding box appears to be a **small object** or region of interest on the ground near some dry vegetation. The scene depicts a rural environment with **hay and shrubs**. In the background, a building is partially obscured by trees. Scattered objects or debris are present on the ground.

Step 2: Understand modality correspondence. In the event modality images, red dots indicate regions with decreasing brightness, while blue dots indicate increasing brightness. The modality following the RGB images exhibits characteristics of the **event** modality, confirming this assignment. In the **first event** image, the green-bounded area corresponds to a mixed red-blue dot region, indicating **dynamic brightness** changes within the area. However, the red-blue pattern does not **differ significantly** from its surroundings, suggesting that the target remains **static**. In **subsequent** images, the target slightly shifts to the **left**. The event modality shows **large clusters** of red-blue points across the background, including outlines of the stationary building, indicating **camera shake**. In the corresponding RGB frames, the small point is evenly distributed, making it **difficult** to discern the target contour clearly.

Step 3: Analyze cross-modal complementarity and verify target location. RGB modality: Provides visual details to determine the target's approximate **location** and **appearance**. Event modality: Indicates that the target is stationary while camera motion causes information **degradation**. The target remains generally static in position, with only minor brightness and activity changes. The event modality confirms the absence of significant **activity** within the target region.

Summarizing the **target position**. In the initial image, the target is **centered** on the ground, blending into the hay. In the second set of images, the target shifts slightly to the **left**. In the final two images, the target position **remains unchanged**. </think>

<answer>[[136,152,21,22], [136,152,21,22], [142,146,18,22], [142,146,18,22], [119,145,37,22], [119,145,37,22]]</answer>

Answer: [[143.35,149.2393,18.8,20.9859], [171.1244,144.7254,13.7187,20.35], [138.1396,148.7903,9.6167,18.6551]]

Figure 11. An example reasoning process of RGB–Event grounding with incorrect predictions. The second and third search images contain grounding errors. The target to be grounded is a chicken.

Images:



Question:

A sequence of images has been input, consisting of alternating modalities images. Your task is to predict the coordinates of the target object in the subsequent images after the first two template images, based on the green bounding boxes [629.0,259.0,58.0,83.0] in these two templates.

RGBX-R1-7B:

<think> Step 1: Identify the target and scene. The target is a man wearing a light-colored top and black trousers, running on a track. He is positioned in the middle of a running formation, with similarly dressed runners both ahead of and behind him. The overall scene is an athletic field.

Step 2: I need to identify the modality beyond RGB. The subsequent frames are grayscale images. All runners in the scene exhibit high grayscale values, especially in the head region, while the nearby track and distant background have lower grayscale values—characteristics consistent with the infrared modality. In the first set of images, the infrared modality clearly delineates the target runner's silhouette, with his head showing higher temperature. His upper body and feet are covered by clothing, resulting in lower grayscale values. In the second set, the target's silhouette remains clear, and his upper body in the infrared modality appears slightly warmer than those of surrounding runners, possibly due to differences in clothing material. The third set shows similar conditions. In the fourth set, the target overlaps with nearby runners; although the infrared modality becomes slightly blurred, the RGB modality still allows identification of his position.

Step 3: In the RGB modality, the target is distinguishable by his light-colored long-sleeved shirt and black trousers, which provide detail contrast against surrounding runners. The infrared modality lacks fine visual details, making it difficult to differentiate the target from nearby runners, but it provides a clear silhouette that verifies the spatial information from RGB.

Combining the observations across frames, the target remains in the middle of the running group, with four to five runners both ahead of and behind him. The target moves forward, and his location can be determined by his relative position within the formation. </think>

<answer>[[718,249,58,83], [718,249,58,83], [681,232,52,73], [681,232,52,73], [676,198,48,55], [676,198,48,55]]</answer>

✓
✓
✗

Answer:
[[741.0,248.0,40.0,82.0], [671.0,229.0,40.0,76.0], [645.0,200.0,35.0,69.0]]

Figure 12. An example reasoning process of RGB–Thermal grounding with incorrect predictions. The third search image contains the grounding error. The target to be grounded is a man.

Images:



Question:

A sequence of images has been input, consisting of alternating modalities images. Your task is to predict the coordinates of the target object in the subsequent images after the first two template images, based on the green bounding boxes [480.0,228.0,81.0,85.0] in these two templates.

RGBX-R1-7B:

<think> Step 1: The target is a black elongated object, possibly a wooden stick or a model. It is being pulled by a person wearing a white top and black trousers. The object is positioned above the person's trousers. The scene is indoors, with dark blue furniture in the background.

Step 2: Identify the modality following RGB. The subsequent images appear mostly black. In the RGB modality, both the person and the chair correspond to dark areas, while a light-gray region appears above the chair, corresponding to a distant hallway in the RGB frames. This matches the principle of the depth modality: regions farther from the camera exhibit higher grayscale values. In the first set of images, the black object appears as a dark region in the depth modality, with edges showing lower grayscale values than the filled area. These edges form a quadrilateral shape consistent with the elongated model. In the second set, the RGB modality shows the object moving to the left side of the chair, and the depth modality reveals a corresponding low-grayscale parallelogram. In the third set, the object returns to its original position from the first image; the depth modality depicts its contour with lower grayscale, and the object appears rotated, increasing its projected area. In the fourth set of images, the object disappears from the frame. No noticeable changes in color or grayscale values are observed in its previous location.

Step 3: In the RGB modality, due to the object's rapid movement, only a blurred shape is visible, but its approximate region can be inferred from motion streaks. In the depth modality, since the object is at a similar distance to the person, most of its area has a grayscale value close to the person's. However, parts of its contour exhibit lower grayscale, aiding identification. In the second image, the object moves to the left of the chair. In the third set, it moves in front of the black trousers, making it harder to observe in RGB due to color overlap. At this point, the depth modality reveals parts of its contour, complementing the faint upper outline from the RGB modality. In the fourth set, the object seems to disappear from the right side of the frame, likely swinging to the height of the person's left hand.

In summary, the object oscillates laterally around the person as its center. In the second image, it moves to the left side of the frame; in the third image, it returns to its initial position; and in the fourth image, it exits the frame from the right. Its overall height remains unchanged. </think>

<answer>[[159,181,75,67], [159,181,75,67], [461,237,130,61], [461,237,130,61], [456,144,64,66], [456,144,64,66]]</answer>

✓
✓
✗

Answer:
[[169.0,188.0,47.0,41.0], [486.0,225.0,100.0,74.0], [472.0,249.0,105.0,91.0]]

Figure 13. An example reasoning process of RGB–Depth grounding with incorrect predictions. The third search image contains the grounding error. The target to be grounded is a notebook.